# Nuclear spin coherence properties of $^{151}\text{Eu}^{3+}$ and $^{153}\text{Eu}^{3+}$ in a $\text{Y}_2\text{O}_3$ transparent ceramic

**J Karlsson[1], N Kunkel[1], A Ikesue[2], A Ferrier[1,3] and P Goldner[1]**

1 PSL Research University, Chimie ParisTech, CNRS, Institut de Recherche de Chimie Paris, 75005, Paris, France
2 World Laboratory, Mutsuno, Atsuta-ku, Nagoya 456-0023, Japan
3 Sorbonne Universités, UPMC Université Paris 06, 75005, Paris, France

E-mail: `jenny.karlsson@chimie-paristech.fr`

**Abstract.** We have measured inhomogeneous linewidths and coherence times ($\text{T}_2$) of nuclear spin transitions in a $\text{Eu}^{3+}$:$\text{Y}_2\text{O}_3$ transparent ceramic by an all-optical spin echo technique. The nuclear spin echo decay curves showed a strong modulation which was attributed to interaction with Y nuclei in the host. The coherence time of the 29 MHz spin transition in $^{151}\text{Eu}^{3+}$ was 16 ms in a small applied magnetic field. Temperature dependent measurements showed that the coherence time was constant up to 18 K and was limited by spin-lattice relaxation for higher temperatures. Nuclear spin echoes in $^{153}\text{Eu}^{3+}$ gave much weaker signals than for the case of $^{151}\text{Eu}^{3+}$. The spin coherence time for the 73 MHz spin transition in $^{153}\text{Eu}^{3+}$ was estimated to 14 ms in a small magnetic field. The study shows that the spin transitions of ceramic $\text{Eu}^{3+}$:$\text{Y}_2\text{O}_3$ have coherence properties comparable to the best rare-earth-doped materials available.

## 1. Introduction

Nuclear spin transitions of rare earth doped crystals are ideal as qubits, the units of quantum information, because they can show long coherence times at low temperatures [1–3]. In addition, rare-earth-doped nuclear spins can be coherently addressed through optical transitions, which have made it possible to realize optical memories with spin storage [4–7] and high fidelity single qubit and gate operations [8–10].

In particular, the nuclear spin transitions of $Eu^{3+}$ in $Y_2SiO_5$ can have population lifetimes of several days and coherence times $T_{2n}$ of tens of ms, which are about one order of magnitude longer than the optical coherence times [11–13]. In addition, by applying coherence control techniques like specific magnetic fields and trains of rf pulses, $T_{2n}$ can be extended to hundreds of ms at low magnetic field [13] and to 6 hours at higher fields [1]. These results suggest for example that long storage time optical quantum memories could be obtained in this system [5]. Although there are several crystals that are currently investigated for applications in quantum information processing with rare earth ions, $Eu^{3+}$ nuclear spin coherence lifetimes have only been reported so far in $Y_2SiO_5$ bulk single crystals.

In this paper, we report on the nuclear spin properties of $Eu^{3+}$ in $Y_2O_3$, which can be obtained not only as single crystals, but also transparent ceramics and nanocrystals. In all these forms, very narrow optical linewidths (1-100 kHz) have been demonstrated [14–19], which make this material interesting for quantum technologies. Moreover, transparent ceramics and nanocrystals represent attractive alternatives to single crystals. For example, $Y_2O_3$ transparent ceramics of large volumes and high optical quality are much easier to obtain than single crystals [20], whereas nanocrystals can be used for efficient single ion detection [21, 22] and coupling to other nanoscale quantum systems for hybrid quantum devices. Measurements were performed with an all-optical technique on a transparent ceramic of $Eu^{3+}$:$Y_2O_3$ that had previously shown long optical coherence lifetimes [18, 19]. We found nuclear spin coherence lifetimes for the two europium isotopes in the range from 14 ms to 16 ms under magnetic fields of a few mT. These values are comparable to the longest ones observed in rare earth doped crystals, i.e. $^{151}Eu^{3+}$ in $Y_2SiO_5$ ($T_{2n}$ = 15-20 ms [12, 13]) and $^{145}Nd^{3+}$:$Y_2SiO_5$ ($T_{2n}$ = 9 ms [3]), which suggests that nuclear spins in $Eu^{3+}$:$Y_2O_3$ could be used as optically addressable, long lived qubits.

## 2. Sample

The investigated sample was a transparent ceramic of $Eu^{3+}$:$Y_2O_3$ containing 0.5 at.% $Eu^{3+}$. It was prepared according to the procedure described in [17] but using 99.999% pure $Y_2O_3$ and $Eu_2O_3$ powders. The sample is described further in [19], contained no sintering additive and was not thermally processed after hot isostatic pressing. These materials are polycrystalline with crystallite size of about 2 $\mu$m as determined by optical microscopy.

Eu$^{3+}$ is replacing Y$^{3+}$ in the crystal lattice and can occupy two sites in cubic $Y_2O_3$ with $C_2$ and $S_6$ symmetry respectively. All experiments were performed on the $C_2$ symmetry site where electric dipole transitions are stronger.

Eu$^{3+}$ has two almost equally abundant isotopes, $^{151}$Eu and $^{153}$Eu, both with nuclear spin $I = 5/2$. The $^7F_0$ ground state as well as the $^5D_0$ excited state in both isotopes are split up into three doubly degenerate hyperfine levels by a nuclear quadrupole interaction with the electric field gradient in the crystal. Figure 1 shows the spin level structure of the two isotopes and the optical transition used in this study [23]. The ordering of the levels is here assumed to be the same as in the case of Eu$^{3+}$:$Y_2SiO_5$, with the smallest splitting between the higher energy levels in the ground state and between the lower energy levels of the excited state. The ordering of the spin levels however does not influence the results and conclusions of this work.
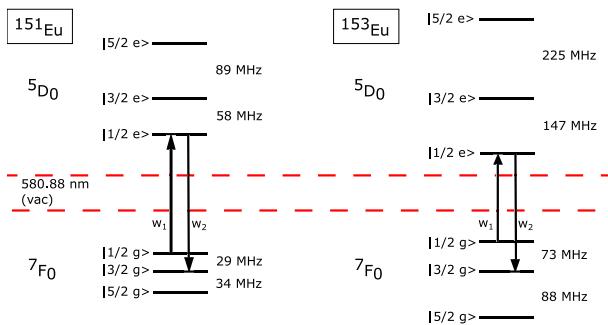


**Figure 1.** Relevant energy levels of $^{151}$Eu$^{3+}$ and $^{153}$Eu$^{3+}$ in $Y_2O_3$. The $^7F_0$ ground state and the $^5D_0$ excited state are split up into three doubly degenerate levels by a nuclear quadrupole interaction. Laser fields at two frequencies $\omega_1$ and $\omega_2$ couple two of the ground state nuclear spin levels to one of the optically excited states. (Color online)

## 3. Method

The sample was placed inside a Janis optical helium bath cryostat and was cooled down to 4 K by a flow of cold helium gas. The temperature was monitored with a temperature sensor attached to the sample surface with thermally conducting grease. The sample could also be kept at higher temperatures, up to 22 K, by fine tuning the helium gas flow and the pressure inside the cryostat. Helmholtz coils sitting outside the cryostat were used to apply magnetic fields up to 6 mT perpendicular to the beam propagation direction.

The beam from a Sirah Matisse dye laser, with a linewidth of approximately 200 kHz and operating at 580.88 nm (vac.), was split into two beams in a polarizing beam splitter and each was sent through an acousto optic modulator, AA Optoelectronic MT200-B100A0,5-VIS, in double pass configuration. The beams were overlapped in a 50/50 beam splitter and focused onto the sample by a 50 mm lens. The transmitted laser beam was aligned onto a photo detector, Thorlabs PDB150A, and the laser power
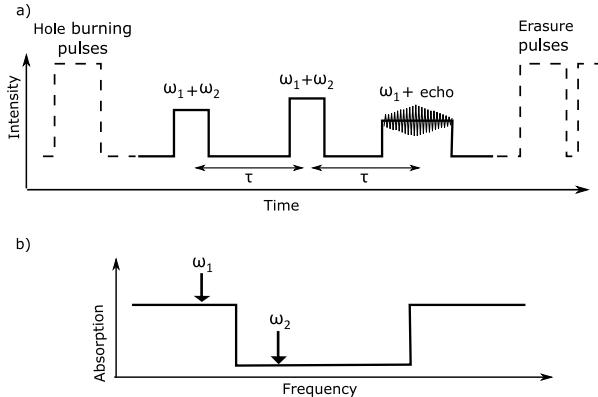
**Figure 2.** a) Pulse sequence used in the spin echo measurement. Two two-color pulses ($\omega_1 + \omega_2$) are used to generate a spin echo. At the time of the spin echo, a third (read) pulse at frequency $\omega_1$ transfers the coherence to the optical transition, which causes an optical emission at frequency $\omega_2$. The echo is detected as a beating in the transmitted light, created by the coherent sum of the read pulse and the optical emission from the ions. b) Before the echo sequence, a spectral hole is burnt within the inhomogeneous absorption profile to create a population difference between the spin levels addressed by the two-color pulses. The read ($\omega_1$) and emitted ($\omega_2$) pulses sit respectively on the side of and inside the spectral hole

incident on the sample was monitored by a second photo detector, Thorlabs PDA10A-EC.

Nuclear spin echoes were generated and detected using an all-optical Raman-scheme [12, 24]. The optical pulse sequence is shown in figure 2 a). A 60 MHz wide spectral hole was first burnt within the inhomogeneous absorption profile to pump the ions into one ground state level, for example the 1/2-spin level, see figures 1 and 2 b). A two-frequency laser pulse ($\omega_1 + \omega_2$) addressing the $^7F_0$-$^5D_0$ optical transition in $Eu^{3+}$ was used to excite a coherence between two ground state spin levels (1/2 and 3/2 in figure 1), separated by $\omega_2$ - $\omega_1$, in a subgroup of ions within the inhomogeneously broadened absorption line. After a wait time $\tau$ another two-frequency pulse was used to flip the phase of the spin coherence. The nuclear spin coherence rephased a time $\tau$ after the second pulse. By applying a single-frequency optical pulse at frequency $\omega_1$, the coherence of the spin levels was transferred into an optical coherence at a frequency $\omega_2$, which caused an optical emission inside the spectral hole. Together with the excitation laser pulse at frequency $\omega_1$ the emission created a beating pattern at the spin transition frequency in the transmitted light [25, 26]. The echo originating from the spin transition was then measured by making a real time fast Fourier transform (FFT) of the signal from the photo detector on an oscilloscope, LeCroy Wavesurfer 24MXs. All pulses were optimized to maximize the echo amplitude for a pulse separation $\tau = 10$ ms, which resulted in 80 $\mu$s long pulses of approximately 20 mW power.

It can be noted that the optical coherence time of the sample is 42 $\mu$s which is short compared to the delay times of several ms used in this work [18]. In addition, since the excitation pulses were much longer than the optimal values for optical echoes,

the beating signal was only related to the spin echoes. This allowed us to detect the spin echo at frequency $\omega_2$, which is the same frequency as the excitation pulses, without overlap with unwanted photon echoes. In previous studies, the coherence of the ground state spin levels was transferred to a different excited state with a laser pulse at a third frequency $\omega_3$ which generated an echo pulse at a forth frequency $\omega_4$, to avoid overlap with photon echoes [27]. Since $Eu^{3+}$ has large hyperfine splittings in the $^5D_0$ excited state (figure 1) this would put high requirements on the bandwidth of the setup. Moreover, with the technique used here, a larger sub-ensemble of ions within the inhomogeneous profile can contribute to the echo, since the laser frequency can match optical transitions to any one of the excited state spin levels. After each echo sequence a series of strong chirped erasure pulses were used to re-shuffle the ions between the ground state levels and prevent permanent hole burning.

## 4. Results

### 4.1. Inhomogeneous linewidth

The inhomogeneous absorption linewidths of the two spin transitions in $^{151}Eu^{3+}$ were measured by tuning the frequency difference $\omega_2$ - $\omega_1$ of the two-color pulses while recording the amplitude of the spin echo, for a fixed pulse separation $\tau = 5$ ms. Lorentzian lines could be fitted to the data and the inhomogeneous linewidth was measured as the FWHM of the fitted curve. The first spin transition was centered at 29.33 MHz, and had a linewidth of 104±5 kHz as shown in figure 3 a). The second spin transition was centered at 33.99 MHz, and the linewidth was 156±13 kHz, see figure 3 c).

The center frequencies are consistent with previously measured transitions in a bulk single crystal [23, 28]. The inhomogeneous linewidths are consistent with the lines measured in [28] and 30-40% narrower than the values given in [23]. The inhomogeneous broadening of the spin transitions is most likely caused by strain in the crystal lattice due to the dopants themselves as well as other impurities and point defects, which, at low concentrations give Lorentzian lineshapes [29]. The difference in inhomogeneous linewidth can then be explained by a difference in doping concentration between the samples, or alternatively by the large uncertainty associated with the method used in [23]. Indeed, the optical inhomogeneous linewidth in our sample is 20 GHz, almost identical to bulk $Eu^{3+}$:$Y_2O_3$ crystals of similar concentration [18, 30], suggesting that no significant additional strain is present in the ceramic.

0.1 % concentrated $Eu^{3+}$:$Y_2SiO_5$ shows inhomogeneous spin transition linewidths of 21 kHz and 38 kHz respectively for the ground state transitions of $^{151}Eu^{3+}$ [13]. This is 4-5 times narrower than the linewidths measured here, which can be explained by the difference in $Eu^{3+}$ concentration which is 5 times lower in the $Y_2SiO_5$ sample. It is also possible that a larger number of intrinsic defects, like oxygen vacancies [19], in the $Y_2O_3$ host material as compared to $Y_2SiO_5$ is responsible for part of the broadening. Indeed,
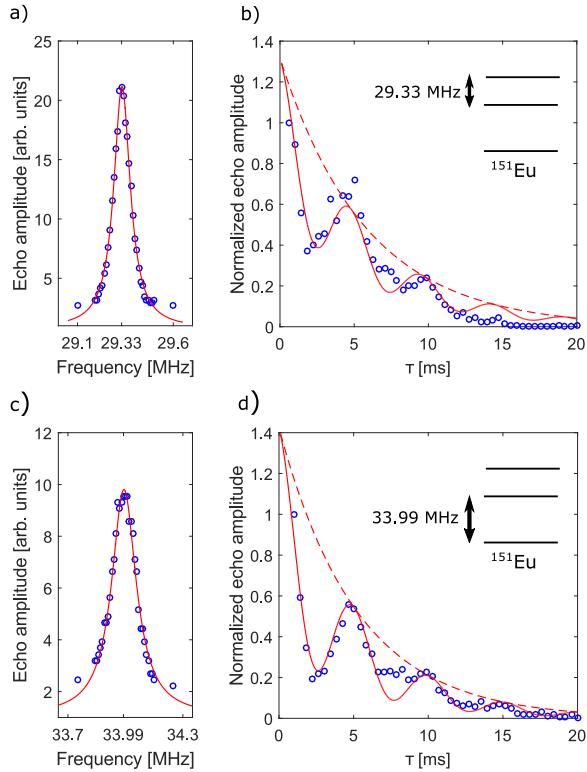
**Figure 3.** Figures a) and c) show the inhomogeneous lines of the spin transitions in $^{151}$Eu, centered at a) 29.33 MHz and c) 33.99 MHz together with fitted Lorentzian curves (red lines). The inhomogeneous linewidths (FWHM) are a) 104±5 kHz and c) 156±13 kHz. Figures b) and d) show typical echo decay curves for b) the 29.33 MHz spin transition and d) the 33.99 MHz spin transition at zero magnetic field. The decays are fitted with an exponential function (red dashed line) modulated by a squared cosine function (red solid line), as described in the text. The coherence times at zero field are 11.6±0.9 ms for the 29.33 MHz transition and 10.5±0.6 ms for the 33.99 MHz transition. (Color online)

the optical inhomogeneous line is about 10 times broader in $Eu^{3+}$:$Y_2O_3$ as compared to $Eu^{3+}$:$Y_2SiO_5$ of similar concentration [11, 18, 30]

## 4.2. Coherence time

The spin echo amplitude was recorded as a function of the pulse separation time, $\tau$, for the 29 MHz transition and the 34 MHz transition respectively, see figure 3 b) and d). The echo decay curves showed a strong echo envelope modulation effect [31] at a frequency of 200 Hz. Very similar echo envelope modulation at 200 Hz has previously been seen in spin echo decays of $Eu^{3+}$:$Y_2SiO_5$ [12, 13]. It was then interpreted as due to the splitting of the $\pm M_I$ hyperfine levels by a small residual magnetic field. A ceramic sample however, as used in this study, contains crystalline regions with all possible orientations relative to an applied magnetic field. As $Eu^{3+}$ ions are located in a site of low symmetry, the nuclear gyromagnetic tensor, which includes an electronic contribution, is expected to be anisotropic, as observed in $Eu^{3+}$:$Y_2SiO_5$ [32]. The magnetic field would then result

in a broadening of the spin inhomogeneous line rather than a well defined splitting. Such a broadening would not give rise to a well defined modulation frequency in the echo decay. Another possible explanation of the observed echo envelope modulation is superhyperfine interaction with $^{89}Y$ nuclear spins (100 % abundance, $I = 1/2$) in the crystal lattice, which has been previously studied in the case of electron spin echoes in $Er^{3+}$:$Y_2SiO_5$ [33].

To investigate these possibilities and determine the coherence time ($T_{2n}$), echo decays were fitted with a function of the form

$$E(\tau) = ae^{-2\tau/T_{2n}}[1 + m\cos^2(\frac{\omega\tau}{2})] \tag{1}$$

shown by the red solid line in figure 3 b) and d). The coherence times were 11.6±0.9 ms and 10.5±0.6 ms for the 29.33 MHz and 33.99 MHz transitions respectively. These values are in the same range as those measured in $Eu^{3+}$:$Y_2SiO_5$ (19 ms at zero magnetic field [13]). This is consistent with a dephasing mechanism dominated by magnetic fluctuations due to yttrium spin flips.

When applying a small magnetic field across the sample, the echo envelope modulation depth decreased and the modulation frequency increased, as shown in figure 4. The modulation frequency increased by 2 kHz/mT up to an applied magnetic field of 0.15 mT, see inset in figure 4. The calculated Larmor frequency of an yttrium ion with a nuclear magnetic moment of 0.14 $\mu_N$ is 2.1 kHz/mT, in good agreement with observation. This indicates that interaction with nearby yttrium nuclei in the crystal lattice is responsible for the observed echo modulation. For higher fields than 0.15 mT it was no longer possible to resolve the modulation (figure 4).

### 4.3. Temperature dependence

To obtain smoother curves with smaller modulation depth and hence more reliable coherence lifetime estimations, a magnetic field of 3 mT was applied across the sample. For magnetic fields larger than 3 mT the signal strength was weaker due to broadening of the inhomogeneous line. The echo decay is slightly non-exponential, which can be seen clearly in figure 5 a) where some decay curves are plotted with a logarithmic y-axis. The non-exponential behavior is a sign of spectral diffusion due to relaxing spins in the crystal lattice surrounding the $Eu^{3+}$ ions. The echo decay can be fitted to a function

$$E(\tau) = E_0 e^{-(2\tau/T_M)^x} \tag{2}$$

where $x$ is a stretch parameter and $T_M$ is the phase memory of the ions [34]. In this case $x = 1.3$ provided the best fit to the data.

At 4 K, the phase memory time $T_M$ of the 29 MHz spin transition increased to 16 ms in a 3 mT field. This is attributed to a slow down of the yttrium spin flip-flop processes in a magnetic field and therefore a lower contribution to $Eu^{3+}$ decoherence, and a possible decrease of the sensitivity of the transition to magnetic field fluctuations [12, 13].
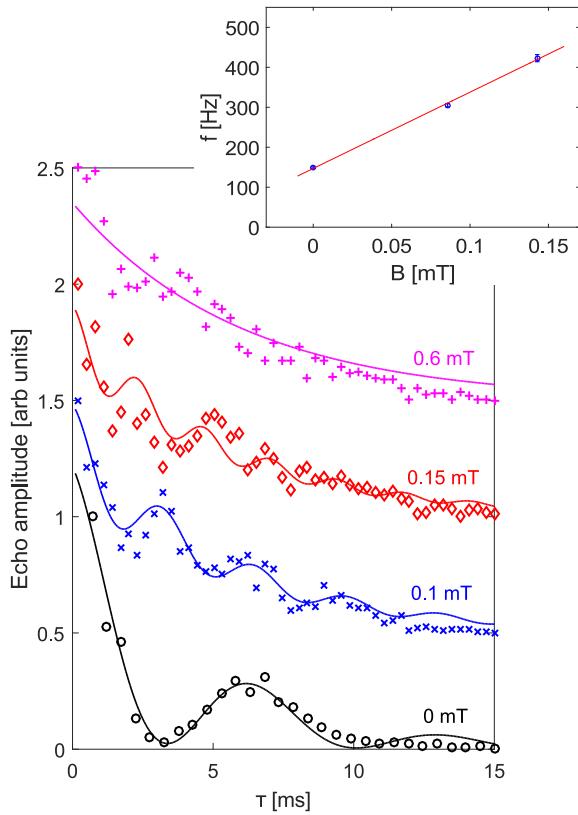
**Figure 4.** Echo decay curves for increasing magnetic fields; no field, 0.1 mT, 0.15 mT and 0.6 mT respectively from the bottom to the top, all recorded at a temperature of 4K. An offset is added to the curves for better visibility. With increasing field the modulation frequency increased and the modulation depth decreased. For applied fields larger than 0.15 mT the oscillation could no longer be resolved and the curve approached an exponential. The inset shows the increase in modulation frequency as a function of applied magnetic field, with a linear slope of 2 kHz/mT. (Color online)

In figure 5 the homogeneous linewidth $\Gamma_h$ of the 29 MHz spin transition is plotted as a function of temperature. The homogeneous linewidth is here calculated from the phase memory time by $\Gamma_h = 1/(\pi T_M)$. The temperature dependence of the homogeneous linewidth fits well to an Orbach process [35] with a temperature independent offset,

$$\Gamma_{Orbach}(T) = A/(e^{\Delta E/kT} - 1) + \Gamma(0), \tag{3}$$

as shown by the red dashed line in figure 5. In the expression above $\Delta E = 199.4$ cm$^{-1}$ is the energy gap to the closest crystal field level above the ground state, $^7$F$_1$ [36]. The model indicates that the coherence time is limited by spin-lattice relaxation for temperatures above 18 K [37]. A least squares fit gives an offset $\Gamma(0) = 20$ Hz ($T_2 = 16$ ms), and Orbach coefficient $A = 1.3 \cdot 10^8$ Hz. As mentioned above, the temperature independent broadening, $\Gamma(0)$, is ascribed to nuclear spin flips of yttrium ions in the crystal lattice.

The constant spin coherence lifetime up to 18 K contrasts with the optical coherence
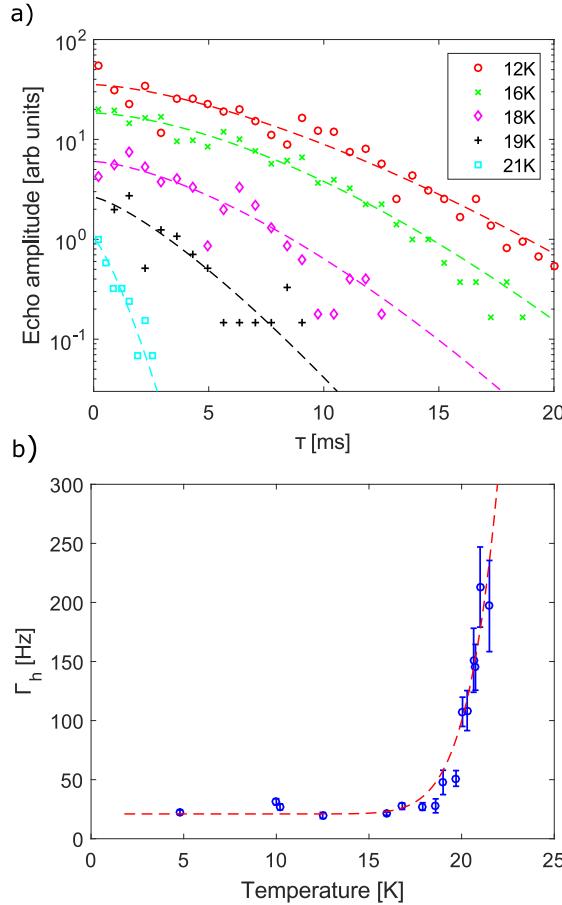
a)

b)



**Figure 5.** Temperature dependence of the homogeneous linewidth, $\Gamma_h$, of the 29 MHz spin transition, with an applied magnetic field of 3 mT. In a) echo decay curves for some different temperatures with a logarithmic y-axis. An offset is added to the curves for increased visibility. The decays are slightly non-exponential which denotes spectral diffusion due to spin flips in the host crystal. The dashed lines are least squares fits to (2). In b) the homogeneous linewidth, $\Gamma_h$, is plotted as a function of temperature. The dashed red line is a fit to the Orbach process with a constant offset of 20 Hz which corresponds to a coherence time of 16 ms up to 18 K. (Color online)

lifetime which is affected by two-phonon Raman processes. As a result, the optical homogeneous linewidth increases as $T^7$ from about 7 K [18]. Long nuclear spin coherence lifetimes at elevated temperatures could nevertheless be useful in schemes where the optical transitions coherences are only used for short times.

## 4.4. Investigations of $^{153}Eu$

$^{153}$Eu has larger energy separation between the nuclear spin levels than $^{151}$Eu. Measuring spin echoes with an all-optical technique in $^{153}$Eu puts higher demands on the bandwidth of the AOMs used. In this study AOMs with bandwiths of 100 MHz were used, which gives 200 MHz tuning range when aligned in double pass configuration. A tuning range of 200 MHz is enough to address both transitions in the ground state of 73 MHz and
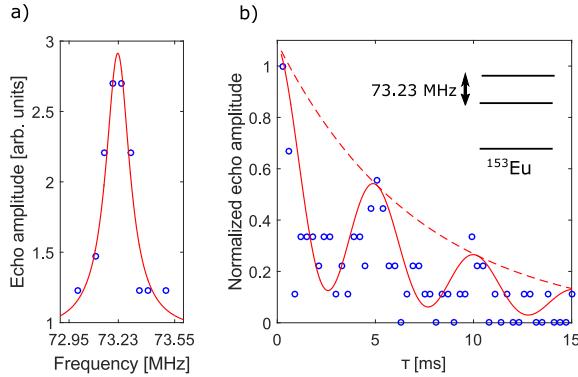
**Figure 6.** a) The inhomogeneous line of one of the spin transitions in $^{153}$Eu, centered at 73.23 MHz together with a fitted Lorentzian curve (red line). The inhomogeneous linewidth (FWHM) is 165±12 kHz. b) The echo decay curve for the same spin transition with an applied magnetic field of 5.7 mT. The decay is fitted with an exponential function (red dashed line) modulated by a squared cosine function (red line). The coherence time is estimated to 14±4 ms. (Color online)

88 MHz respectively [23]. The holeburning and erasure pulses used are however less efficient due to a lower AOM efficiency at large detuning from the center frequency.

Despite the limitations mentioned above it was possible to detect weak spin echoes from the 73 MHz transition. The echo signal was about 30 times smaller than for the case of $^{151}$Eu. For the 88 MHz transition no echo could be detected. One possible explanation of the low echo efficiency can be weaker optical transitions between levels with different spin projections in the ground and excited states (e.g. 1/2e to 3/2g, see figure 1). This would decrease the efficiency of the two-colour excitations and read out scheme.

Figure 6 a) shows the inhomogeneous line of the 73 MHz spin transition in $^{153}$Eu. The peak of the line is found at 73.23±0.01 MHz, consistent with previous results in single crystals [23]. The inhomogeneous linewidth (FWHM) is 165±12 kHz. As discussed above for $^{151}$Eu, this is significantly narrower than the inhomogeneous broadening measured in [23] of 400±100 kHz. It is also expected that the inhomogeneous linewidth scales with the energy of the spin transition. This is in qualitative agreement with our data for $^{151}$Eu and $^{153}$Eu, where the higher energy spin transitions also have larger inhomogeneous linewidths. The scaling is however not linear, which has also been seen in other materials [38].

To measure the echo amplitude as a function of pulse separation a magnetic field of 5.7 mT was applied to the sample, which caused the echo signal to increase by almost a factor of 2, which could be related to an increase in coherence lifetime. For even higher fields the signal was weaker, probably due to broadening of the inhomogeneous line. The coherence time could be estimated to 14±4 ms, as shown in figure 6 b).

All results are summarized in table 1. The 87.8 MHz spin transition in $^{153}$Eu has not been measured in this work.

**Table 1.** Summary of the nuclear spin inhomogeneous lines (peaks $\nu$ and widths $\Delta\nu$), as well as the nuclear spin coherence times ($T_2$) of a $Eu^{3+}$:$Y_2O_3$ transparent ceramic.

| $^{151}$Eu | | |
| --- | --- | --- |
| $\nu$ | 29.33±0.01 MHz | 33.99±0.01 MHz |
| $\Delta\nu$ (FWHM) | 104±5 kHz | 156±13 kHz |
| $T_2$ (no field) | 11.6±0.9 ms | 10.5±0.6 ms |
| $T_2$ (3 mT) | 16±3 ms | - |
| $^{153}$Eu | | |
| $\nu$ | 73.23±0.01 MHz | 87.8±0.2 MHz [23] |
| $\Delta\nu$ (FWHM) | 165±12 kHz | - |
| $T_2$ (no field) | - | - |
| $T_2$ (5.7 mT) | 14±4 ms | - |

## 5. Conclusion

A transparent ceramic sample was used to study the nuclear spin properties of $Eu^{3+}$ ions in $Y_2O_3$. Using an all-optical scheme, nuclear spin echoes could be detected on the 1/2-3/2 and 3/2-5/2 ground state transitions for $^{151}Eu^{3+}$ and on the 1/2-3/2 transition of $^{153}Eu^{3+}$. Inhomogeneous linewidths in the range 104-165 kHz were measured by monitoring the echo amplitude as a function of the excitation frequency. For $^{151}Eu^{3+}$ these values are similar to those of bulk $Y_2O_3$ crystals, indicating similar strain between ceramics and single crystals.

The coherence time of the 29 MHz spin transition in $^{151}$Eu is 12 ms in zero magnetic field and increase to 16 ms in 3 mT. The coherence time is constant up to about 18 K, and is lifetime limited for higher temperatures. These values are similar to those measured in $Eu^{3+}$:$Y_2SiO_5$, which suggests that dephasing is due to $Y^{3+}$ nuclear spin flip-flops. This in turn is promising for applying dephasing control techniques that can increase coherence lifetimes by several orders of magnitude. We also identified an echo envelope modulation effect which was concluded to be due to superhyperfine coupling to nuclear spins of yttrium ions in the host lattice. As was pointed out in [33], this Eu-Y interaction could potentially be used to build multi-qubit systems.

These results show that $Eu^{3+}$:$Y_2O_3$ is a promising system to design optically addressable qubits with long lifetimes. This study also shows that long nuclear spin coherence lifetimes can be observed in samples with micron size crystalline domains. An especially interesting question for further investigations is wether spin coherence are preserved in the $Eu^{3+}$:$Y_2O_3$ nanocrystals that show narrow optical linewidths.

## Acknowledgments

## References

[1] Zhong M, Hedges M P, Ahlefeldt R L, Bartholomew J G, Beavan S E, Wittig S M, Longdell J J and Sellars M J 2015 *Nature* **517** 177–180

[2] Fraval E, Sellars M J and Longdell J J 2005 *Phys. Rev. Lett.* **95**(3) 030506 URL http://link.aps.org/doi/10.1103/PhysRevLett.95.030506

[3] Wolfowicz G, Maier-Flaig H, Marino R, Ferrier A, Vezin H, Morton J J L and Goldner P 2015 *Phys. Rev. Lett.* **114**(17) 170503 URL http://link.aps.org/doi/10.1103/PhysRevLett.114.170503

[4] Lovrić M, Suter D, Ferrier A and Goldner P 2013 *Phys. Rev. Lett.* **111**(2) 020503 URL http://link.aps.org/doi/10.1103/PhysRevLett.111.020503

[5] Jobez P, Laplane C, Timoney N, Gisin N, Ferrier A, Goldner P and Afzelius M 2015 *Phys. Rev. Lett.* **114**(23) 230502 URL http://link.aps.org/doi/10.1103/PhysRevLett.114.230502

[6] Gündoğan M, Ledingham P M, Kutluer K, Mazzera M and de Riedmatten H 2015 *Phys. Rev. Lett.* **114**(23) 230501 URL http://link.aps.org/doi/10.1103/PhysRevLett.114.230501

[7] Heinze G, Hubrich C and Halfmann T 2013 *Phys. Rev. Lett.* **111**(3) 033601 URL http://link.aps.org/doi/10.1103/PhysRevLett.111.033601

[8] Longdell J J and Sellars M J 2004 *Phys. Rev. A* **69**(3) 032307 URL http://link.aps.org/doi/10.1103/PhysRevA.69.032307

[9] Rippe L, Julsgaard B, Walther A, Ying Y and Kröll S 2008 *Phys. Rev. A* **77**(2) 022307 URL http://link.aps.org/doi/10.1103/PhysRevA.77.022307

[10] Longdell J J, Sellars M J and Manson N B 2004 *Phys. Rev. Lett.* **93**(13) 130503 URL http://link.aps.org/doi/10.1103/PhysRevLett.93.130503

[11] Könz F, Sun Y, Thiel C W, Cone R L, Equall R W, Hutcheson R L and Macfarlane R M 2003 *Phys. Rev. B* **68**(8) 085109 URL http://link.aps.org/doi/10.1103/PhysRevB.68.085109

[12] Alexander A L, Longdell J J and Sellars M J 2007 *J. Opt. Soc. Am. B* **24** 2479–2482 URL http://josab.osa.org/abstract.cfm?URI=josab-24-9-2479

[13] Arcangeli A, Lovrić M, Tumino B, Ferrier A and Goldner P 2014 *Phys. Rev. B* **89**(18) 184305 URL http://link.aps.org/doi/10.1103/PhysRevB.89.184305

[14] Macfarlane R M and Shelby R M 1981 *Optics Communications* **39** 169–171

[15] Perrot A, Goldner P, Giaume D, Lovrić M, Andriamiadamanana C, Gonçalves R R and Ferrier A 2013 *Physical Review Letters* **111** 203601

[16] Bartholomew J G, de Oliveira Lima K, Ferrier A and Goldner P 2016 Toward bulk crystal coherence ttime in eu$^{3+}$:y$_2$o$_3$ nanocrystals *CLEO:QELS Fundamental Science*

[17] Ferrier A, Thiel C W, Tumino B, Ramirez M O, Bausá L E, Cone R L, Ikesue A and Goldner P 2013 *Physical Review B* **87** 041102

[18] Kunkel N, Ferrier A, Thiel C W, Ramirez M O, Bausá L E, Cone R L, Ikesue A and Goldner P 2015 *APL Materials* **3** 096103

[19] Kunkel N, Bartholomew J, Binet L, Ikesue A and Goldner P 2016 *Journal of Physical Chemistry C* **120** 13725–13731

[20] Ikesue A and Aung Y L 2008 *Nature Photonics* **2** 721 – 727

[21] Kolesov R, Xia K, Reuter R, Stöhr R, Zappe A, Meijer J, Hemmer P and Wrachtrup J 2012 *Nature communications* **3** 1029

[22] Utikal T, Eichhammer E, Petersen L, Renn A, Götzinger S and Sandoghdar V 2014 *Nature communications* **5** 3627

[23] Babbitt W R, Lezama A and Mossberg T W 1989 *Physical Review B* **39** 1987–1992

[24] Hartmann S 1968 *IEEE Journal of Quantum Electronics* **4** 802–807

[25] Mlynek J, Wong N C, DeVoe R G, Kintzer E S and Brewer R G 1983 *Phys. Rev. Lett.* **50**(13) 993–996 URL `http://link.aps.org/doi/10.1103/PhysRevLett.50.993`

[26] Wong N C, Kintzer E S, Mlynek J, DeVoe R G and Brewer R G 1983 *Phys. Rev. B* **28**(9) 4993–5010 URL `http://link.aps.org/doi/10.1103/PhysRevB.28.4993`

[27] Beaudoux F, Guillot-Noël O, Lejay J, Ferrier A and Goldner P 2012 *Journal of Physics B* **45** 124014

[28] Yamaguchi M and Suemoto T 2003 *Journal of the Physical Society of Japan* **72** 429–436

[29] Stoneham A M 1969 *Rev. Mod. Phys.* **41**(1) 82–108 URL `http://link.aps.org/doi/10.1103/RevModPhys.41.82`

[30] Flinn G P, Jang K W, Ganem J, Jones M L, Meltzer R S and Macfarlane R M 1994 *Physical Review B* **49** 5821–5827

[31] Rowan L G, Hahn E L and Mims W B 1965 *Physical review* **137** 61–71 URL `http://journals.aps.org/pr/pdf/10.1103/PhysRev.137.A61`

[32] Longdell J J, Alexander A L and Sellars M J 2006 *Phys. Rev. B* **74**(19) 195101 URL `http://link.aps.org/doi/10.1103/PhysRevB.74.195101`

[33] Guillot-Noël O, Vezin H, Goldner P, Beaudoux F, Vincent J, Lejay J and Lorgeré I 2007 *Physical Review B* **76** 180408

[34] Mims W B 1968 *Phys. Rev.* **168**(2) 370–389 URL `http://link.aps.org/doi/10.1103/PhysRev.168.370`

[35] Orbach R 1961 *Proceedings of the Royal Society of London A: Mathematical, Physical and Engineering Sciences* **264** 458–484 ISSN 0080-4630 (*Preprint* `http://rspa.royalsocietypublishing.org/content/264/1319/458.full.pdf`) URL `http://rspa.royalsocietypublishing.org/content/264/1319/458`

[36] Chang N C and Gruber J B 1964 *The Journal of Chemical Physics* **41** 3227–3234 URL `http://scitation.aip.org/content/aip/journal/jcp/41/10/10.1063/1.1725701`

[37] Arcangeli A, Macfarlane R M, Ferrier A and Goldner P 2015 *Physical review B* **92** 224401

[38] Lovric M, Glasenapp P, Suter D, Tumino B, Ferrier A, Goldner P, Sabooni M, Rippe L and Kröll S 2011 *Physical Review B* **84** 104417